Biochimica et Biophysica Acta 1828 (2013) 2032–2040

Contents lists available at SciVerse ScienceDirect

Biochimica et Biophysica Acta

journal homepage: www.elsevier.com/locate/bbamem

Membrane protein interactions between different *Arabidopsis thaliana* MRS2-type magnesium transporters are highly permissive

Johanna Schmitz [1], Alena Tierbach, Henning Lenz, Karoline Meschenmoser [2], Volker Knoop *

IZMB — Institut für Zelluläre und Molekulare Botanik, Abteilung Molekulare Evolution, Universität Bonn, Kirschallee 1, D-53115 Bonn, Germany

ARTICLE INFO

Article history:
Received 29 November 2012
Received in revised form 6 May 2013
Accepted 22 May 2013
Available online 31 May 2013

Keywords:
2-TM-GxN proteins
mbSUS
Cation channel
I-TASSER protein modelling

ABSTRACT

Membrane proteins of the *Arabidopsis thaliana* MRS2 (MGT) family have been characterised as magnesium transporters. Like their bacterial CorA homologues, the plant MRS2 proteins are characterised by an invariable GMN tripeptide motif terminating the first of two closely spaced transmembrane domains at the carboxy-termini. The functional Mg^{2+} transport channel is assembled as a pentamer in the case of CorA. However, in contrast to the single CorA genes of bacteria, plant genomes encode up to 10 highly divergent MRS2 proteins. To elucidate structure–function relationships and the possibility of plant MRS2 hetero-pentamer formation, we performed protein–protein interaction studies in the yeast mating-based split-ubiquitin system (mbSUS) and concomitant protein modelling using I-TASSER. Despite very restricted sequence similarities and variable polypeptide insertions all AtMRS2 proteins feature the key structural elements determined for the CorA crystal structure. The mbSUS setup conclusively demonstrates protein–protein interactions of any given AtMRS2 protein not only with itself but also highly permissive interactions to varying degrees among all AtMRS2 proteins. AtMRS2-3 seems particularly prone to non-selective, strong interactions with the other homologues. Deletion constructs show that six amino acids may be deleted from the carboxy-terminus and 27 (but not 41) from the amino-terminus of AtMRS2-7 without impairment of homologous or heterologous protein interactions. Despite significant diversification, the plant MRS2 proteins have obviously retained an ancient CorA/MRS2 core structure and the capacity for protein–protein interactions. Plant magnesium homeostasis may be influenced by hetero-oligomer channel formation where different plant MRS2 proteins meet in the same membrane naturally or in transgenic approaches.

1. Introduction

The well-characterised bacterial CorA proteins, as well as the yeast ALR and MRS2 proteins and their homologues in other eukaryotes, such as the extended MRS2 (=MGT) gene families of plants, are structurally homologous magnesium transport proteins [1]. These proteins universally exhibit two carboxy-terminally located α-helical transmembrane (TM) stretches connected with a short, ca. 10 amino acid long polypeptide loop, which invariably carries a conserved glycine–methionine–asparagine (GMN) tripeptide motif at the end of the first TM domain. Consequently, we suggested the label 2-TM-GMN proteins for this super-class of CorA/ALR/MRS2-like proteins present in all domains of life. An extended 2-TM-GxN superfamily additionally encompasses more distantly related proteins with variants of the GMN motif, like GIN and GVN, which are likely involved in the transport of zinc and cadmium, respectively [2].

The gene and protein designations in yeast and bacteria reflect the initially observed phenotypes (e.g. CorA: cobalt resistance, MRS2: mitochondrial RNA splicing, ALR: aluminium resistance or MNR: manganese resistance) when the respective genes encoding 2-TM-GMN proteins are defect or over-expressed [3–7]. Their key function, however, is obviously the transport of Mg^{2+} across biological membranes, as conclusively demonstrated by their ability to complement defects of magnesium transport in respective mutants of the diverse genetic systems even across wide phylogenetic distances [8–14]. Moreover, a high-conductance (~155 pS) Mg^{2+} flux was demonstrated directly in single-channel patch clamping experiments of MRS2 in giant lipid vesicles [15,16]. The MRS2 channel proved to be specific for Mg^{2+} with significantly lowered conductance for Ni^{2+} and no evidence for the transport of Ca^{2+}, likely explained by the dehydrated Mg^{2+} ion being the smallest of all biological relevant cations. On the other hand, the strictly hexa-coordinated Mg^{2+} ion experiences a 400-fold volume expansion upon hydration, which makes it the largest of all hydrated cations and necessitates unique mechanisms for removal of its hydration shell prior to channelling through biological membranes [17].

X-ray crystallography has demonstrated that the functional *Thermotoga maritima* Mg^{2+} transport channel assembles as a CorA protein pentamer with the respective first TM domains of the five subunits lining the membrane pore [18–22]. In contrast to the single CorA

* Corresponding author. Tel.: +49 228 73 6466; fax: +49 228 73 6467.
E-mail address: volker.knoop@uni-bonn.de (V. Knoop).
[1] New address: Albrecht-von-Haller-Institut für Pflanzenwissenschaften, Abteilung Molekularbiologie und Physiologie der Pflanze, Georg-August-Universität, Julia-Lermontowa-Weg 3, D-37077 Göttingen, Germany.
[2] New address: Pallas Healthcare Consulting GmbH, Knesebeckstr. 30, D-10623 Berlin, Germany.

0005-2736/$ – see front matter © 2013 Elsevier B.V. All rights reserved.
http://dx.doi.org/10.1016/j.bbamem.2013.05.019

proteins encoded in most bacterial genomes, 2-TM-GMN proteins are much more diversified in eukaryote genomes. Two proteins each exist in the yeast plasma-membrane (ALR1 and ALR2) and in the inner mitochondrial membrane (MRS2 and LPE10), respectively. In plant genomes, the genes encoding homologous proteins have diversified yet more and we have labelled the members of the resulting gene family in *Arabidopsis thaliana* as "AtMRS2" genes given the initially observed complementation of the yeast MRS2 mutant [10]. The alternative labelling "MGT" for the gene family has been proposed near-simultaneously and has since been used in parallel [11,13,23–25]. It must be noted, however, that the plant MRS2 ("MGT") genes are *not* homologous to the bacterial Mgt genes MgtA/B and MgtE, which encode proteins of entirely different structural makeup for alternative, inducible magnesium transport pathways in (some) bacteria [26].

The diversity of the circa ten highly divergent plant MRS2 proteins encoded in the genomes of flowering plants (angiosperms) led us to explore whether they would likely have retained key structural elements of CorA and assemble similarly. The possibility that different plant MRS2 proteins could assemble as hetero-pentamers for channel formation when targeted to the same membrane compartment seemed particularly intriguing. We used the yeast mating-based split ubiquitin system (mbSUS) [27–30] to study protein–protein interactions of the *A. thaliana* AtMRS2 proteins (see Fig. 2). Concomitantly, we used the "Iterative Threading Assembly Refinement" service I-TASSER to explore protein structure predictions for the AtMRS2 proteins [31,32].

2. Materials and methods

2.1. Construct design

Coding regions of AtMRS2 genes for cloning into split-ubiquitin constructs were obtained with PCR approaches amplifying AtMRS2 cDNA sequences with gene-specific oligonucleotide primers. Oligonucleotides were 5′-extended to include the 36 nt. long B1 linker sequence (ACAAGTTTGTACAAAAAAGCAGGCTCTCCAACCACC) in the upstream primer and the 39 nt. long B2 linker sequence (TACCCAGCTTTCTTGTA CAAAGTGGTTGGTGGTGGCGGA, as reverse complement) in the downstream primer for in vivo homologous recombination cloning in yeast. Accordingly, the B1 and B2 sequences translate into oligopeptide spacer sequences TSLYKKAGSPTT and YPAFLYKVVGGGG linking the AtMRS2 coding regions to the upstream or downstream ubiquitin moieties, respectively. The complete list of full oligonucleotide primer sequences is available from the authors upon request.

2.2. In vivo recombination cloning

PCR products were inserted into vectors pNXgate33-3HA, pXNgate21-3HA and pMetYCgate by in vivo recombination in yeast with linearized vector plasmids cut within (or flanking) the vectors' kanamycin (KanMX) cassette located between the B1 and B2 motifs [33,34]. The N-terminal ubiquitin moiety consists of the first 34 amino acids of the full length protein and carries an amino acid exchange (I13G) in pNXgate33-3HA and pXNgate21-3HA, which precludes its spontaneous self-assembly with the C-terminal ubiquitin half (Cub) representing amino acid 35 to 76 of the full length ubiquitin. In the following, this mutated "NubG" moiety is referred to as "Nub" for simplicity. Cub constructs in pMetYCgate were cloned in haploid yeast strain THY.AP4 (of mating type a) and Nub constructs cloned in pNXgate33-3HA or pXNgate21-3HA were cloned in haploid yeast strain THY.AP5 (of mating type α). Both yeast strains are auxotroph for biosynthesis of adenine (*ade2*), histidine (*his3*), leucine (*leu2*) and tryptophan (*trp1*) and THY.AP4 carries an additional uracil auxotrophy (*ura3*). The co-transformation of PCR products (>200 ng) and linearized vectors (>50 ng) into freshly prepared competent yeast cells in the presence of lithium acetate followed the published procedures for efficient yeast transformation [35]. Selection of successful transformants was based on tryptophan autotrophy restored by the Nub-containing plasmids in THY.AP5 and on leucine autotrophy restored by pMetYCgate in THY.AP4. Plasmids were isolated from yeast clone cultures and transformed into *Escherichia coli* for re-isolation and control sequencing of the constructs before mating experiments were performed. Sequencing was performed commercially by GATC Biotech GmbH (Konstanz, Germany) or by Macrogen Inc. (Seoul, South Korea), respectively. Sequence handling was done using the MEGA software [36].

2.3. Mating and detection of protein interaction

Haploid yeast strains THY.AP4 (of mating type a) containing the Cub constructs cloned into pMetYCgate and THY.AP5 (of mating type α) containing the Nub constructs cloned into pNXgate33-3HA or pXNgate21-3HA were mated according the updated published protocols [33]. Upon successful mating the resulting diploid yeasts were selected on SC media lacking leucine, tryptophan, uracil and methionine (see Figs. 2 and 3). In order to detect protein–protein interactions of Nub and Cub constructs, diploid yeast clones were replica-stamped onto agar plates with SD (synthetic dropout) media additionally lacking adenine and histidine in a series of increasing concentrations of methionine (0, 10, 20, 40 and 60 μM) to suppress the expression of Cub constructs under the control of the pMet25 promoter. Because of the reporter gene constructs provided in yeast strain THY.AP4 restoring adenine (ADE2) and histidine (HIS3) autotrophy and *lacZ* encoding β-galactosidase, successful protein interaction will become detectable on SD media (see Fig. 2). All three reporter genes are under the control of the lexA promoter, which can be induced by the artificial PLV (ProtA/LexA/VP16) transcription factor after its liberation from the Cub moiety upon functional interaction with the Nub part. Alternatively, protein–protein interaction was monitored by an X-Gal overlay test of diploid yeasts growing on the selective SC plates as published [33]. Wild-type Nub constructs without the I13G mutation were included as positive controls since they assemble also in the absence of protein–protein interaction partners and the empty pXNgate vector was included as a negative control since an upstream stop codon should preclude expression of the ubiquitin moiety when not fused to an upstream protein sequence.

2.4. In silico analyses of AtMRS2 protein structures

Full length AtMRS2 protein sequences were uploaded to the I-TASSER (Iterative Threading Assembly Refinement) server at http://zhanglab.ccmb.med.umich.edu/I-TASSER for structural predictions with standard settings (i.e. without any additional restraints or a priori exclusions for modelling). Essentially, I-TASSER uses a four-step procedure to combine alignment-based modelling of available protein structure with ab initio modelling of non-aligned regions in a protein query to ultimately offer a selection of top-scoring protein models [32,31]. The resulting protein models were inspected and visualised using PyMOL 1.5.0.3 (http://www.pymol.org, "The PyMOL Molecular Graphics System", Schrödinger, LLC) and self-prepared scripts. Given that the automatic update routine for the I-TASSER template library excluded full-length structures due to sequence identity when partial structures had been included previously, the recent full length CorA structure of *Methanocaldococcus jannaschii* PDB (Protein Data Bank) entry 4EV6 was kindly added manually upon our request. The homologous CorA protein structure of *T. maritima* used for comparison (see Fig. 1) is PDB entry 2IUB.

3. Results

3.1. Characterising AtMRS2 protein structures

The universal conservation of two carboxyterminal transmembrane stretches TM1 and TM2 with the former ending in the universally

conserved GMN tripeptide motif and the capacity for functional complementation suggested that plant and yeast MRS2 proteins and the bacterial CorA proteins are structurally and functionally homologous. Primary amino acid sequence similarities among the eukaryotic MRS2 and to the bacterial CorA proteins are extremely low, however (see Suppl. Fig. 1). To explore whether the plant MRS2 protein sequences

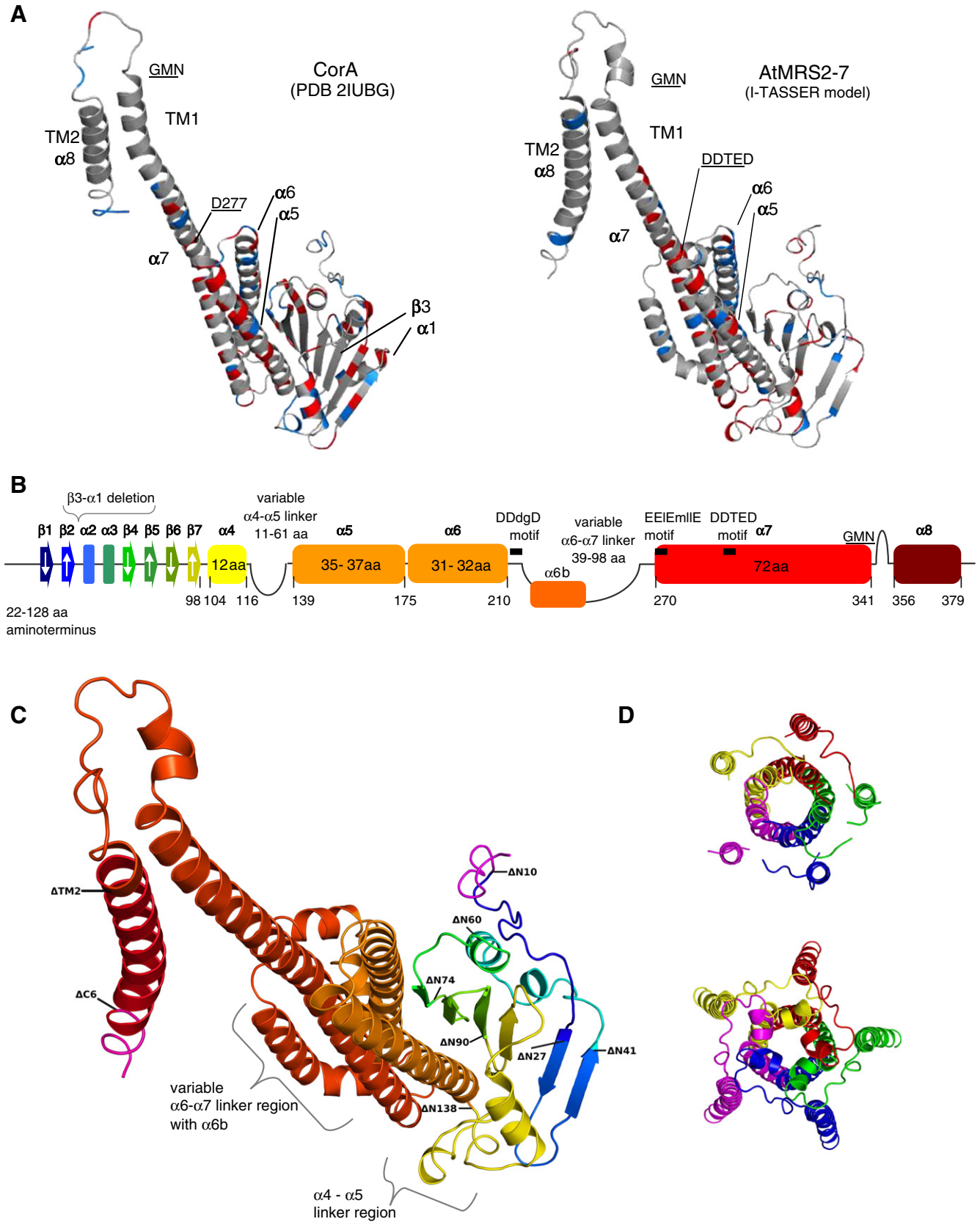

would likely fold into structures analogous or at least similar to the recently determined CorA protein crystal structures [19,20,18], we used the I-TASSER (Iterative Threading Assembly Refinement) WWW server [31,32] to predict structures for the *A. thaliana* AtMRS2 proteins. Using the full length AtMRS2 protein sequences, we found that in all cases, the best structural similarities were indeed found with the recently determined bacterial CorA protein structures, those of the ZntB zinc efflux transporters [37,38] or of the respective partial structures including those of the yeast MRS2 protein, which are known to have 2-TM-GxN structures.

The predicted succession of β-pleated sheets and α-helical secondary structure elements, which make up the large N-terminal funnel structure in the assembled pentamers, is largely identical among the AtMRS2 proteins and to the known CorA structure (Fig. 1). The structural models for all AtMRS2 proteins consistently feature a conserved 72 aa long α7 "stalk" helix that includes transmembrane stretch TM1 at its end, which terminates in the universally conserved GMN motif as exemplarily shown for AtMRS2-7 (Fig. 1A). A highly variable loop region connects to the conserved α-helix 8 representing TM2. The "willow" helices α5 and α6 of the CorA structure [19] are likewise universally conserved in all AtMRS2 homologues. Notably, in all AtMRS2 protein models only a short "elbow" sequence connects between α5 and the "swivel" helix α6 (Fig. 1 A and B), which likely has a crucial role in channel opening and closing in CorA [20,39,40].

In contrast to CorA, however, the two conserved willow helices α5 and α6 of the plant MRS2 proteins are embedded between highly variable and extended polypeptide regions linking them to the respective upstream and downstream α-helices 4 and 7 (Fig. 1C). The long α6–α7 linker in particular carries variably extended α-helical regions in the plant proteins, here designated as α6b. Nevertheless, the unequivocal structural matches between the plant MRS2 homologues and CorA also include AtMRS2-3, which is characterised by particular large sequence insertions between the alpha-helical regions α4 and α5 and between α6 and α7, as well as AtMRS2-11, which in contrast is characterised by a very long amino-terminal extension and a deletion between α6 and α7, respectively.

Like in CorA, a set of short β-pleated sheets is sandwiched between two sets of α-helices at the amino-termini of the AtMRS2 proteins. However, secondary structures corresponding to β3 and α1 of CorA are missing in all AtMRS2 proteins and make the AtMRS2 beta-sheet arrays β2–β1–β7–β6–β5–β4 completely anti-parallel in comparison to CorA, where the additionally inserted β3 beta-sheet runs parallel to β7 (Fig. 1B and C). Intriguingly, the arrangement of the beta sheet array also differs to varying extent in the recently determined yeast MRS2 cytosolic domain (PDB entry 3RKG) or the *M. jannaschii* CorA structure (Suppl. Fig. 2).

Interestingly, several amino acid residues conserved in the bacterial CorA proteins that were discussed as important for CorA function are not conserved in the AtMRS2 proteins. This includes proline P303, which introduces a kink in the middle of CorA TM1. Aspartate D277 which has been discussed as a key residue marking the cytoplasmic end of the pore where it widens into the funnel [18,39] is the last residue of the DDTED motif in the AtMRS2 proteins (Fig. 1A). Likewise, the universal GMN motif is embedded in a YGMNF sequence environment and the following periplasmatic loop region (which notably remained undetermined due to a disordered state in the *Thermotoga* CorA X-ray crystal structures) carries a highly conserved MPEL sequence in many bacterial CorA proteins [41–43], but neither of these motifs is present in the plant homologues. Two pairs of residues (T305–M302 and L294–M291) within TM1 have been described as constrictions to create two small cavities in the narrow CorA pore. Of these, however, only L294 is highly conserved in the corresponding positions of the AtMRS2 proteins, likely being the key residue creating a barrier at the cytoplasmic entrance of the pore, an observation nicely fitting to a mutational study demonstrating the relevance of L294 for gating of the Mg^{2+} channel [44]. Finally, two aspartate residues (D89 in α3 and D253 in α7) were identified as likely coordinating Mg^{2+} ions between two adjacent CorA polypeptides in the assembled pentamers [19,39,45]. Neither of the two is conserved in the corresponding positions of the plant proteins, however. Interestingly though, an aspartate is universally present three residues (i.e. approximately one helical turn) upstream in α3 of the AtMRS2 proteins and the latter is close to a glutamate-rich motif containing slightly less conserved methionines and leucines (EElEmllE) at the start of the stalk α-helix 7 (Fig. 1B). In conclusion, all AtMRS2 proteins show a very good overall fit with the X-ray crystal structures determined for the bacterial CorA homologue but differ significantly in detail with respect to conservation of several residues that have been discussed as critical for CorA functionality previously [39].

3.2. AtMRS2-mbSUS construct cloning

We cloned the full set of functional *A. thaliana* MRS2 proteins as fusions to the carboxy-terminal (Cub) and amino-terminal (Nub) halves of split ubiquitin via in vivo recombination cloning in yeast. Due to a single-nucleotide indel, AtMRS2-8 is a frame-shifted pseudogene in the widely used ecotype Columbia (Col-0) but functional in some other ecotypes whereas AtMRS2-9 appears to be a pseudogene in all *Arabidopsis* ecotypes investigated so far (H. Lenz, unpublished observations). Hence, we used the complete set of nine functional AtMRS2 genes of *Arabidopsis* ecotype Col-0 plus AtMRS2-8, which was replaced by its functional counterpart from ecotype Landsberg (Ler).

The ten AtMRS2 gene coding regions were fused at their downstream ends in frame with the carboxy-terminal ubiquitin half (Cub) and, reciprocally, to the amino-terminal half of split ubiquitin (Nub). The latter constructs were created as fusions of Nub to the amino-terminal ends of all ten AtMRS2 proteins (Nub-AtMRS2-x) and, in parallel, alternatively to their carboxy-terminal ends (AtMRS2-x-Nub). Consequently, ten full length AtMRS2-x-Cub constructs were ultimately employed in matings with two different sets of ten respective Nub-constructs each. Previous studies had found that fusions of Nub to the amino-termini of respective target proteins generally resulted in stronger indications of protein–protein interactions in the mbSUS setup than the Nub-fusions to their carboxy-termini [33,46].

Fig. 1. A: The AtMRS2 protein structures predicted by I-TASSER as exemplarily shown for AtMRS2-7 (right) in comparison to the *Thermotoga* CorA structure determined by X-ray crystallography (left) reveal structural homology. Blue and red colouring indicate basic and acidic side chains and key structural elements including transmembrane (TM) domains and the conserved GMN tripeptide motif are labelled. B: The suite of secondary structure motifs in AtMRS2 proteins and CorA is largely identical. Exceptions are a short N-terminal β-sheet and an α-helix motif (β3–α1) present in CorA but lacking in the AtMRS2 homologues (rendering the β-sheet succession in the latter completely anti-parallel) and the highly length-variable α4–α5 and α6–α7 linker regions in the AtMRS2 proteins. The small black bars indicate short polypeptide stretches rich in aspartate (D) and glutamate (E), which are conserved among the AtMRS2 proteins and may participate in creating a negatively charged sink in the assembled funnel structure. Different colours are analogous to the rainbow-colouring from blue to red also used in panel C to display the succession of structural motifs from N- to C-terminus. Size ranges are indicated for the different members of the AtMRS2 family above and amino acid positions are indicated below the respective structural elements using AtMRS2-7 as a reference (see suppl. Fig. S1) C: Rainbow colour display of the AtMRS2-7 protein highlighting the variable linker regions lacking homologies in CorA and the extent of successive deletions in the mbSUS protein interaction studies. D: Conceptual assembly of the magnesium transport channel for AtMRS2-7 (bottom) assuming the same five-fold rotational symmetry as for CorA (top). Different colours (red, green, blue, purple, yellow) are used for the five respective subunits. Shown is an "outside view" on the transmembrane regions perpendicular to the membrane plane, facing the external short loop sequences. AtMRS2 proteins may differ from CorA by a small additional *a*-helical stretch in the short external loop sequences and by a "kink" in the TM2 domain which bends them into the surrounding membrane regions.

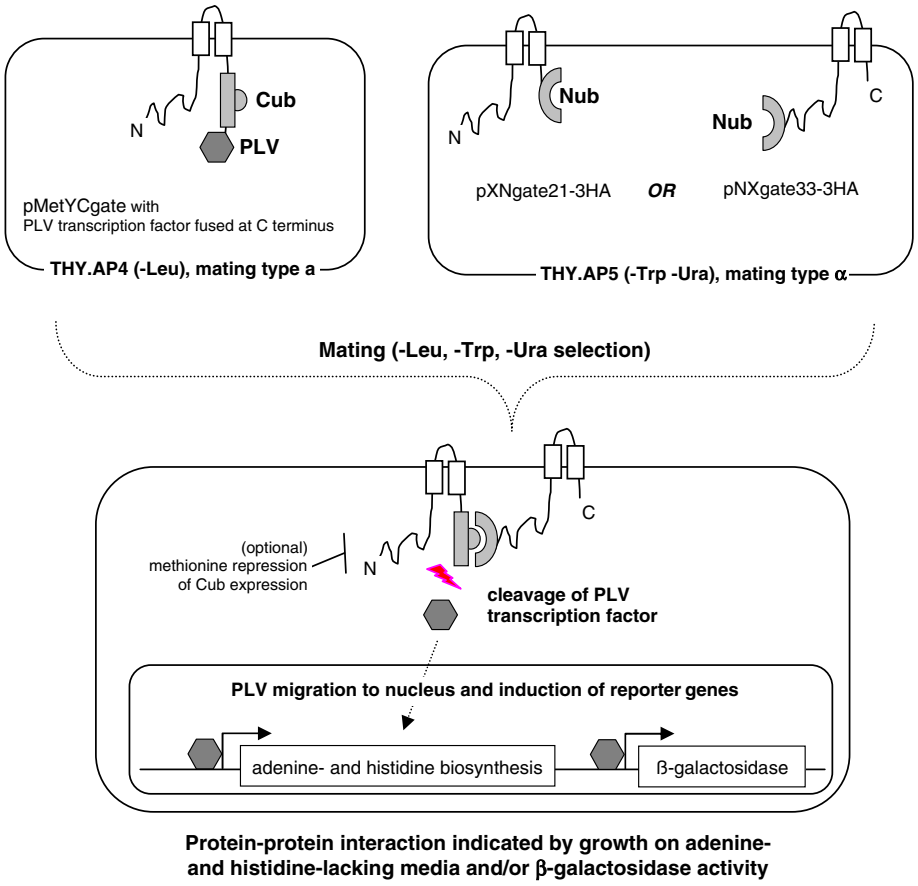

Fig. 2. Strategy of mbSUS as applied for identification of protein–protein interactions between AtMRS2 proteins. AtMRS2 proteins are characterised by a long N-terminus rich in α-helical domains and two carboxyterminal TM domains. AtMRS2 coding sequences are linked to the carboxy-terminal half of split ubiquitin (Cub, amino acids 35–76) followed by the artificial transcription factor PLV in vector pMetYCgate. Reciprocally, the amino-terminal half of split ubiquitin (Nub, amino acids 1–34) is fused either to the N-terminus (in vector pNXgate33-3HA) or to the C-terminus (in vector pXNgate21-3HA) of the AtMRS2 coding sequences. The mutated "NubG" moiety used in the mbSUS setup carries a single amino acid exchange in comparison to wild-type ubiquitin (I13G) to abolish spontaneous re-assembly with the Cub part.

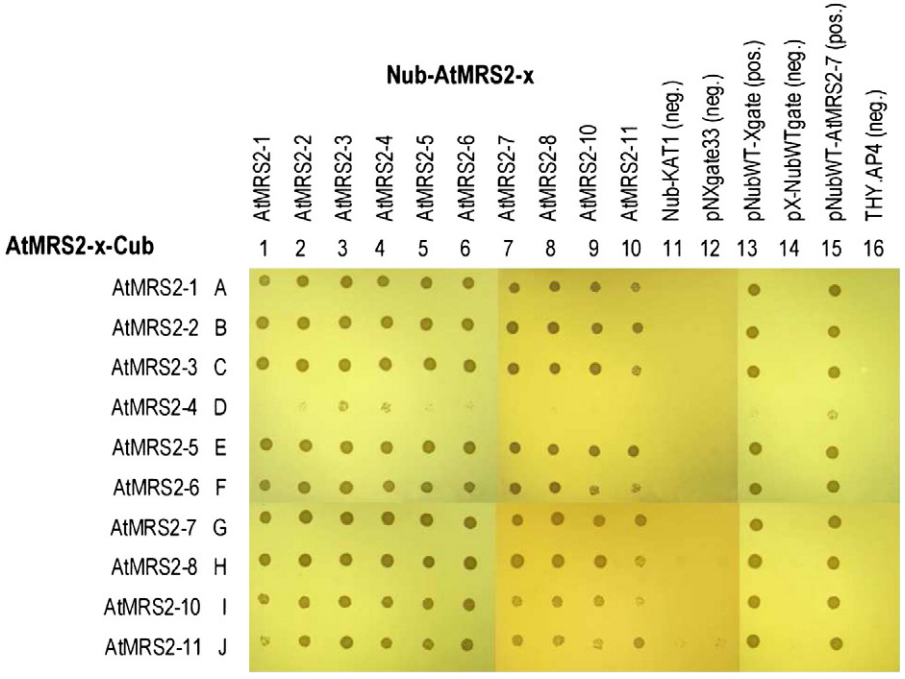

Fig. 3. Results of growing diploid yeast strains obtained via mating of AtMRS2-x-Cub constructs (lines A–J) with Nub-AtMRS2-x constructs (columns 1–10) on SD media selecting for interaction of the respective AtMRS2-x partners. Included as positive controls for interaction of the Cub constructs are the wild-type Nub construct alone (column 13) and in fusion with AtMRS2-7 (column 15), respectively. The haploid THY.AP4 strain (column 16), the empty Nub construct vectors (columns 12, 14) and a Nub-fusion of the potassium transport channel KAT1 (column 11) were included as negative controls. The complete set of interaction patterns observed under increased concentrations of methionine to repress Cub construct expression is given in Supplementary Fig. 3.

3.3. Mating assays

Upon mating the haploid yeast strains containing Cub constructs (THY.AP4 mating type a) with those containing the different Nub constructs (THY.AP5, mating type α), we consistently obtained viable yeasts growing under the appropriate selective conditions for diploid strains (i.e. SC plates lacking leucine, tryptophan, uracil and methionine). Accordingly, we investigated a total number of 200 mating combinations of AtMRS2 Cub- and Nub-constructs plus the respective negative and positive controls in the mbSUS setups. The resulting diploid yeast strains could subsequently be tested under selective conditions to investigate protein–protein interactions of the respective Cub- and Nub-constructs (for the full set of different selective conditions see Supplementary Figs. 3–5).

Under the conditions selecting for protein–protein interactions (i.e. SD plates additionally lacking adenine and histidine) all AtMRS2-Cub constructs except AtMRS2-4-Cub indicated protein–protein interactions with all Nub-AtMRS2 constructs and with the positive control (i.e. wild-type Nub) to varying degrees (Fig. 3). Homologous and heterologous interactions already appear somewhat weaker for AtMRS2-1, AtMRS2-10 and AtMRS2-11 (lines A, I and J and columns 1, 9 and 10, respectively, in Fig. 3), which was subsequently confirmed with the further experimentation as outlined below. Interestingly, even in the absence of a strong signal for the positive control interaction with wild-type Nub (D13), the AtMRS2-4-Cub construct revealed weak interactions with the wild-type Nub fused to AtMRS2-7 (D15), in the homologous pairing with Nub-AtMRS2-4 (D4) and also in the heterologous pairing with Nub-AtMRS2-3 (D3), which was subsequently shown to be particularly permissive for interaction.

All results indicating protein–protein interactions (except for AtMRS2-4) are fully consistent when compared with the independent reciprocal matings of Cub- and Nub-fusions "mirrored" along a diagonal line (i.e. A1 to J10 in Fig. 3) joining the respective homologous pairings: For example, similarly weak interactions are observed in the mating of AtMRS2-11-Cub with Nub-AtMRS2-10 (J9) and reciprocally of AtMRS2-10-Cub with Nub-AtMRS2-11 (I10).

The above results for protein–protein interactions observed with the Nub-AtMRS2 constructs are conclusively supported when the Nub moiety is fused alternatively to the carboxy-termini instead of the amino-termini of AtMRS2 proteins in the resulting AtMRS2-Nub constructs (Fig. 4). As has been observed previously [34,47], this order of translational fusion (i.e. AtMRS2-x-Nub, Fig. 4) consistently shows significantly weaker interactions with the Cub constructs than the amino-terminal Nub fusions (Nub-AtMRS2-x, Fig. 3). The homologous interactions become very weak or even undetectable for AtMRS2-10, AtMRS2-11 and AtMRS2-1 (lines A, I and J and columns 1, 9 and 10 in Fig. 4). Notably, the AtMRS2-4-Nub fusion reveals a different result when the Nub moiety is now fused to the carboxy- instead of the amino-terminus of AtMRS2-4. No significant interactions are seen for AtMRS2-4-Nub (Fig. 4, column 4), which thus behaves very similar to the AtMRS2-4-Cub, but unlike the Nub-AtMRS2-4 construct (Fig. 3, column 4). The accessible native amino-terminus in the AtMRS2-4-Nub and AtMRS2-4 Cub constructs may cause the majority of the protein products to get mis-targeted to the mitochondria in the yeast, where they become unavailable for interactions with the respective partners or preclude cleavage and liberation of the transcription factor and its migration to the nucleus. AtMRS2-4 is predicted to be chloroplast-localised but its closest phylogenetic relative, AtMRS2-6 has been shown to be mitochondrially targeted in planta [25]. On the other hand, the AtMRS2-6 constructs do not show similar evidence for potential mitochondrial targeting in the mbSUS setup, likely indicating different functionality of organelle targeting signals in the heterologous yeast environment. Certainly, a possible destabilising of relevant protein structures upon addition of ubiquitin modules may be a remote alternative possibility to explain missing interaction signals.

The propensity of AtMRS2-3 to permissively engage in heterologous protein–protein interactions (including the weakly interacting proteins AtMRS2-1, AtMRS2-10 and AtMRS2-11) becomes yet more

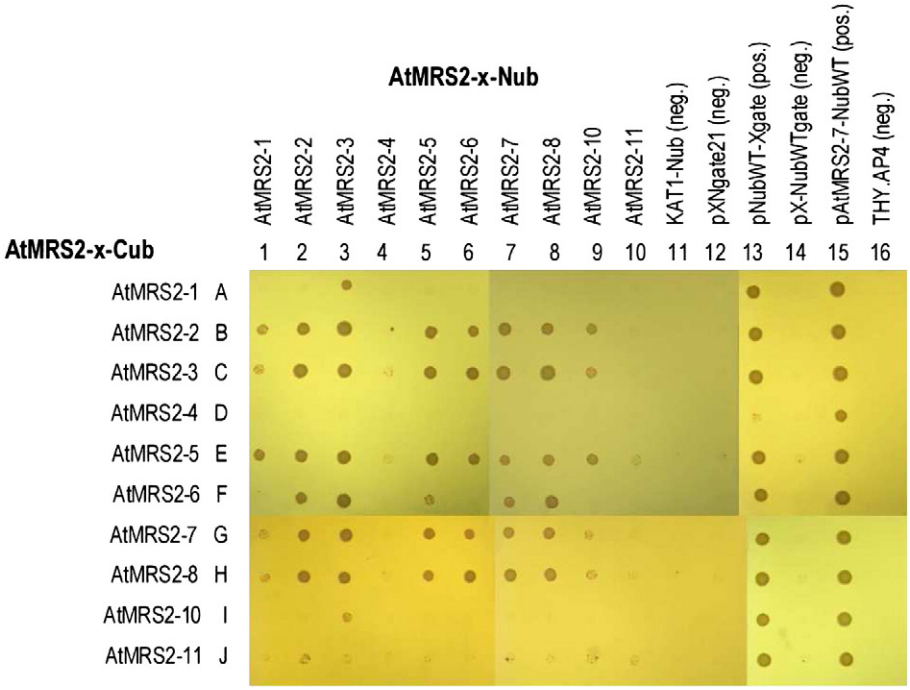

Fig. 4. Results of growing diploid yeast strains obtained via mating of AtMRS2-x-Cub constructs (lines A–J) with AtMRS2-x-Nub constructs (columns 1–10) on SD media selecting for interaction of the respective AtMRS2-x partners. Included as positive controls for interaction of the Cub constructs are the wild-type Nub construct alone (column 13) and in fusion with AtMRS2-7 (column 15), respectively. The haploid THY.AP4 strain (column 16), the empty Nub construct vectors (columns 12, 14) and a Nub-fusion of the potassium transport channel KAT1 (column 11) were included as negative controls. The complete set of interaction patterns observed under increased concentrations of methionine to repress Cub construct expression is given in Supplementary Fig. 4.

pronounced under the structurally less favourable conditions with the Nub moieties fused carboxy-terminally (line C and column 3, respectively, in Fig. 4). This is similarly observed when expression of the Cub-constructs is repressed by adding increasing amounts of methionine to the selective media (Suppl. Figs. 3 and 4).

3.3.1. Towards identifying structures mediating protein–protein interaction

Given the conclusive results for the full-length Cub and Nub fusions of AtMRS2 genes, we wished to investigate whether the mbSUS setup could subsequently be used to define AtMRS2 protein structures relevant for protein–protein interactions more precisely. To this end, we focussed on AtMRS2-7 given its clearly demonstrated important physiological role for developing plants growing in low-magnesium environments [9]. We created AtMRS2-7 constructs with serially progressing deletions from the amino-terminus in Cub fusion constructs and from the carboxy-terminus in the Nub fusion constructs, respectively. These constructs were used in reciprocal matings among each other and with the full length AtMRS2-7 constructs. Additionally, we also included the full length AtMRS2-3 and AtMRS2-11 constructs to check whether the partially deleted AtMRS2-7 constructs would show a change in interaction patterns with partners that previously showed particularly strong (AtMRS2-3) or weak (AtMRS2-11) propensities for heterologous interactions. The results are shown in Fig. 5 and Supplemental Fig. 5.

As previously seen, all constructs containing the Nub moiety fused to the amino-terminus (odd-numbered columns 1, 3, 5, 7 and 9 in Fig. 5) consistently show much stronger interaction with the respective Cub-partners than those with Nub instead fused to the carboxy-terminus (even-numbered columns 2, 4, 6, 8 and 10 in Fig. 5). Obviously, a deletion of 10 or 27 amino acids from the AtMRS2-7 N-terminus (lines A–C in Fig. 5) neither impairs the homologous nor the heterologous protein–protein interactions, whereas further deletions of 41, 60, 74, 90 or 138 amino acids (lines D–H in Fig. 5) abolish the capacity for such interactions.

Similarly, the last six carboxy-terminal amino acids of AtMRS2-7 just up to the end of its second transmembrane domain (AtMRS2-7ΔC6) can be deleted without impairing the ability for protein–protein interactions (columns 3 and 4 in Fig. 5). Notably, the results obtained with the AtMRS2-7 deletion constructs are entirely independent of considering interactions with AtMRS2-7 itself or considering the strong or weak heterologous interactions with AtMRS2-3 or AtMRS2-11, respectively, the latter of which is only clearly detectable without methionine repression (Suppl. Fig. 5). Moreover, the matings of the amino-terminally or carboxy-terminally truncated AtMRS2-7 constructs give consistent results independent of using the full-length or deletion constructs shortened from respective other protein end as mating partners. Both clearly define the relevant AtMRS2-7 protein structures to be located between amino acids 28 and 380.

As a further test we also included Nub constructs deleting the carboxy-terminal transmembrane domain completely (columns 5 and 6 in Fig. 5) by ubiquitin fusions created within the loop region between the transmembrane domains (see Suppl. Fig. 1). In these constructs, it is questionable whether the remaining first TM domain alone would allow for proper membrane insertion. Interestingly, no detectable interaction was seen for the AtMRS2-7-ΔTM2-Nub construct (column 6), which would upon membrane insertion place the Nub domain on the other side of the membrane, precluding interaction with any Cub construct. Conversely, the corresponding Nub-AtMRS2-7-ΔTM2 construct indeed shows some weak and promiscuous interactions with Cub partners (column 5), either due to membrane targeting with only the TM1 domain and/or the presence of the resulting, freely diffusible construct in the cytosol.

4. Discussion

The here reported modelling studies clearly reveal a convincing structural homology of the AtMRS2 proteins with the X-ray crystal structures lately determined for the bacterial CorA-type proteins. The striking overall structural similarities despite only very limited primary sequence similarities (see Suppl. Fig. 1) are fully in line with the previously demonstrated capacity for functional complementation of different proteins in the 2-TM-GMN family even across

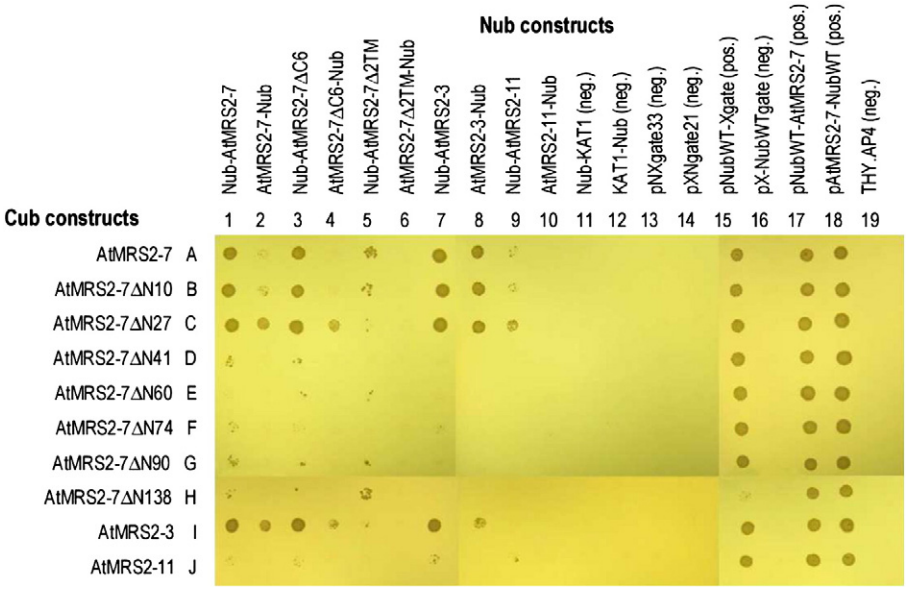

Fig. 5. Results of growing diploid yeast strains obtained via mating of AtMRS2-x-Cub constructs (lines) with AtMRS2-x-Nub constructs (columns) on SD media selecting for interaction of the respective AtMRS2-x partners including 20 μM methionine. Different full length and amino-terminal (lines A–H) and carboxy-terminal (columns 1–6) deletion constructs of AtMRS2-7 and the respective full-length partners interacting permissively (AtMRS2-3, line I and columns 7–8) or non-permissively (AtMRS2-11, line J, columns 9–10), respectively, are also included. Included as positive controls for interaction of the Cub constructs are the wild-type Nub construct alone (column 15) and in fusion with AtMRS2-7 (columns 17 and 18), respectively. The haploid THY.AP4 strain (column 19), the empty Nub construct vectors (columns 13, 14 and 16) and a Nub-fusion of the potassium transport channel KAT1 (columns 11 and 12) were included as negative controls. The complete set of interaction patterns observed under increased concentrations of methionine to repress Cub construct expression is given in Supplementary Fig. 5.

wide phylogenetic distances. Consistently, the recent successful functional reconstitution of AtMRS2-10 in proteoliposomes revealed CorA-like transport properties and specificities [48]. However, the *A. thaliana* MRS2 proteins seem to differ from CorA in structural details. The absence of one short β-sheet and one α-helical motif in the N-terminal β-sheet assembly of the funnel and the highly sequence-variable polypeptide insertions between the "willow"-helices α5 and α6 are the most notable of these differences. It is interesting to note that the *M. jannaschii* CorA crystal structure determined only very recently [49], like the plant MRS2 proteins, similarly lacks one α-helical and one β-sheet stretch at its N-terminus (Suppl. Fig. 2). Intriguingly, the reference CorA protein of *T. maritima* has now been characterised as a cobalt rather than bona fide magnesium transporter [50,51], a finding that deserves attention and may suggest that alternative divalent cations need to be kept in mind as potential CorA transport substrates. The in planta studies of MRS2 proteins have so far not provided any evidence for transport of ions other than magnesium but any structural differences in detail or the assembly of functional transport channels as either homo-pentamers or hetero-pentamers involving different MRS2 proteins could certainly extend the spectrum of divalent cations being transported.

In the light of the above considerations it is interesting to note that several key residues previously discussed as crucial for CorA structure and gating functions are absent in the AtMRS2 homologues. One case in point is the MPEL tetrapeptide motif conserved among the overwhelming majority of bacterial CorA proteins that is located in the short ca. 10 amino acid long loop sequence connecting the two TM domains and which likely determines the extracellular channel pore entry to initially recognise a hydrated Mg^{2+} ion [43]. It is interesting to remember that the loop sequence between the two TM domains remained undetermined in the *Thermotoga* CorA X-ray crystal structure likely due to a disordered state. In contrast, the inter-TM-loop was completely resolved in the recently determined *M. jannaschii* CorA crystal structure and the GMN motif could be located at the bottom of a concave pore opening [49]. The *M. jannaschii* CorA homologue belongs to the much smaller group of CorA proteins with an LPLA tetrapeptide motif replacing the MPEL in most bacterial homologues. However, neither of the two tetrapeptide motifs is present in any plant MRS2 protein and similarly several negatively charged residues implied in attraction and binding of Mg^{2+} and in gating and regulating of the CorA pore opening have no exact counterparts in the homologous plant MRS2 funnel structures.

We have used the yeast mbSUS to investigate protein–protein interactions between the ten functional MRS2-type magnesium transport proteins of *A. thaliana*. The results from the yeast mating experiments are internally consistent and all our assays revealed stronger interactions when the Nub moiety is fused to the amino-terminus rather than to the carboxy-terminus of the respective target proteins, as has been seen before [33]. We observed homologous protein–protein interaction of each protein with itself but also found widely permissive heterologous interactions among the different proteins of the AtMRS2 family. In accord with our findings, homologous and heterologous interactions have previously also been observed using the mbSUS approach for the closely related yeast ALR1 and ALR2 proteins [52]. Despite significant protein sequence variability and extensions (notably a long amino-terminus in AtMRS2-11) or insertions (particularly around willow helices α5 and α6 in AtMRS2-3), the capacity for protein–protein interaction for channel assembly is retained. Independent of homologous or heterologous interactions, we observed a wide spectrum of protein–protein interaction strengths, ranging from a particularly strong propensity for homologous or heterologous interactions in the case of AtMRS2-3 to significantly lower strengths of protein–protein pairing in the case of the most ancestral protein of the family, AtMRS2-11. It is particularly intriguing to remember that AtMRS2-3 carries long polypeptide insertions in the critical regions embedding the two conserved "willow" helices α5 and α6 into the remaining protein structure. Structural alterations like these as well as the non-conservation of certain residues discussed as functionally crucial for the CorA structure make further investigations of the plant MRS2 homologues all the more interesting.

Deletion constructs of AtMRS2-7 show that the same MRS2 protein regions obviously mediate homologous and heterologous protein–protein interactions. Both the first 27 amino acids from the amino-terminus and the end of the protein behind the 2nd TM domain could be deleted in our mbSUS experiments without abolishing the capacity for such protein–protein interactions. Hence, the mbSUS system seems to be very well suited to further identify the relevant AtMRS2-protein structures that mediate assembly of the channel in the membrane in yet more detail. It is worth to remember that the yeast MRS2 and ALR1 proteins carry significantly extended N- and C-termini; in fact, ALR1 at 859 aa is more than twice as long as the bacterial CorA counterparts. Massive deletions of these ALR1 extensions were not found to impact the Mg^{2+} transport capacity [53]. We consider it likely that the conserved secondary structure elements beginning with the anti-parallel β-sheet arrangement (Fig. 1) are crucial both for assembly and transport functionality of 2-TM-GxN proteins.

The option of combinatorial AtMRS2 hetero-oligomer formation would vastly increase the number of different magnesium channel pentamer assemblies with potentially different transport properties in plants. Obviously, this could be welcome adaptations in sessile organisms like plants to differentially regulate magnesium homeostasis in development or in response to different nutrient availabilities. However, in no single case did we find that a particular combination of two different AtMRS2 proteins would be stronger than the respective homologous interactions of the two proteins under consideration. This observation at least indicates that a formation of AtMRS2 hetero-pentamers is not a priori necessary for assembly of stable AtMRS2 channels in the plant cell membranes. Similarly, although all AtMRS2 proteins showed the capacity for permissive heterologous interactions in the mbSUS setup to certain degrees, these are very likely only partly relevant in the natural situation in plant cells in any case, given that simultaneous expression in the same tissues and targeting to the same membranes would be a prerequisite.

The five-fold rotational symmetry of the magnesium transporters consisting of five CorA proteins has been puzzling given the strict octahedral coordination of six water molecules in the inner hydration shell of the Mg^{2+} ion. The recently determined structure of a *Thermotoga* CorA mutant in an "unlocked" state has revealed asymmetric binding of a partially dehydrated Mg^{2+} ion with three of five GMN motifs at the channel entrance and with two of five monomer serines (S284) within the channel close to the cytoplasmic exit [22]. Hence, any asymmetric assembly of CorA/MRS2-like magnesium channels from different subunits is at least principally compatible with the transport process. In the case of the yeast mitochondrial homologues MRS2 and LPE10, it was found that co-expression of both genes is needed to complement the corresponding double mutant and co-immunoprecipitation indeed supports the idea of hetero-oligomeric channel formation [54].

Irrespective of the natural in planta situation, the hetero-oligomerization of different MRS2 proteins is relevant for over-expression and/or intentional MRS2 mis-targeting strategies in engineering transgenic plants towards altered physiologies of magnesium uptake and homeostasis. Given the interplay of magnesium and aluminium in plant nutrition, the alleviation of aluminium toxicity in acidic soils by over-expression of magnesium transporters is among the most interesting perspectives of such transgenic approaches [5,23,55].

Supplementary data to this article can be found online at http://dx.doi.org/10.1016/j.bbamem.2013.05.019.

Acknowledgement

We are very grateful to Petr Obrdlik (now at IonGate Biosciences Frankfurt, Germany) for very helpful advice on the yeast mbSUS and

who kindly provided the necessary vectors and yeast strains. We also wish to express our gratitude to the colleagues at I-TASSER for establishing this valuable bioinformatic tool and especially to Drs. Yang Zhang and Mitra Pralay (Ann Arbor, MI, USA) for the friendly and helpful exchange and their courtesy to manually load the full *M. jannaschii* CorA structures into the template library while this manuscript was under revision.

References

[1] A.S. Moomaw, M.E. Maguire, The unique nature of Mg^{2+} channels, Physiology 23 (2008) 275–285.
[2] V. Knoop, M. Groth-Malonek, M. Gebert, K. Eifler, K. Weyand, Transport of magnesium and other divalent cations: evolution of the 2-TM-GxN proteins in the MIT superfamily, Mol. Genet. Genom. 274 (2005) 205–216.
[3] G. Wiesenberger, M. Waldherr, R.J. Schweyen, The nuclear gene MRS2 is essential for the excision of group II introns from yeast mitochondrial transcripts in vivo, J. Biol. Chem. 267 (1992) 6963–6969.
[4] S.P. Hmiel, M.D. Snavely, C.G. Miller, M.E. Maguire, Magnesium transport in *Salmonella typhimurium*: characterization of magnesium influx and cloning of a transport gene, J. Bacteriol. 168 (1986) 1444–1450.
[5] C.W. MacDiarmid, R.C. Gardner, Overexpression of the *Saccharomyces cerevisiae* magnesium transport system confers resistance to aluminum ion, J. Biol. Chem. 273 (1998) 1727–1732.
[6] N.P. Pisat, A. Pandey, C.W. MacDiarmid, MNR2 regulates intracellular magnesium storage in *Saccharomyces cerevisiae*, Genetics 183 (2009) 873–884.
[7] B.M. Waters, Moving magnesium in plant cells, New Phytol. 190 (2011) 510–513.
[8] D.M. Bui, J. Gregan, E. Jarosch, A. Ragnini, R.J. Schweyen, The bacterial magnesium transporter CorA can functionally substitute for its putative homologue Mrs2p in the yeast inner mitochondrial membrane, J. Biol. Chem. 274 (1999) 20438–20443.
[9] M. Gebert, K. Meschenmoser, S. Svidová, J. Weghuber, R. Schweyen, K. Eifler, H. Lenz, K. Weyand, V. Knoop, A root-expressed magnesium transporter of the *MRS2/MGT* gene family in *Arabidopsis thaliana* allows for growth in low-Mg^{2+} environments, Plant Cell 21 (2009) 4018–4030.
[10] I. Schock, J. Gregan, S. Steinhauser, R. Schweyen, A. Brennicke, V. Knoop, A member of a novel *Arabidopsis thaliana* gene family of candidate Mg^{2+} ion transporters complements a yeast mitochondrial group II intron-splicing mutant, Plant J. 24 (2000) 489–501.
[11] L. Li, A.F. Tutone, R.S. Drummond, R.C. Gardner, S. Luan, A novel family of magnesium transport genes in *Arabidopsis*, Plant Cell 13 (2001) 2761–2775.
[12] G. Zsurka, J. Gregán, R.J. Schweyen, The human mitochondrial Mrs2 protein functionally substitutes for its yeast homologue, a candidate magnesium transporter, Genomics 72 (2001) 158–168.
[13] J. Chen, L.G. Li, Z.H. Liu, Y.J. Yuan, L.L. Guo, D.D. Mao, L.F. Tian, L.B. Chen, S. Luan, D.P. Li, Magnesium transporter AtMGT9 is essential for pollen development in *Arabidopsis*, Cell Res. 19 (2009) 887–898.
[14] R.S.M. Drummond, A. Tutone, Y.C. Li, R.C. Gardner, A putative magnesium transporter AtMRS2-11 is localized to the plant chloroplast envelope membrane system, Plant Sci. 170 (2006) 78–89.
[15] R. Schindl, J. Weghuber, C. Romanin, R.J. Schweyen, Mrs2p forms a high conductance Mg^{2+} selective channel in mitochondria, Biophys. J. 93 (2007) 3872–3883.
[16] O. Dalmas, Magnesium selective ion channels, Biophys. J. 93 (2007) 3729–3730.
[17] M.E. Maguire, J.A. Cowan, Magnesium chemistry and biochemistry, Biometals 15 (2002) 203–210.
[18] S. Eshaghi, D. Niegowski, A. Kohl, D.M. Molina, S.A. Lesley, P. Nordlund, Crystal structure of a divalent metal ion transporter CorA at 2.9 angstrom resolution, Science 313 (2006) 354–357.
[19] V.V. Lunin, E. Dobrovetsky, G. Khutoreskaya, R. Zhang, A. Joachimiak, D.A. Doyle, A. Bochkarev, M.E. Maguire, A.M. Edwards, C.M. Koth, Crystal structure of the CorA Mg^{2+} transporter, Nature 440 (2006) 833–837.
[20] J. Payandeh, E.F. Pai, A structural basis for Mg^{2+} homeostasis and the CorA translocation cycle, EMBO J. 25 (2006) 3762–3773.
[21] D. Niegowski, S. Eshaghi, The CorA family: structure and function revisited, Cell. Mol. Life Sci. 64 (2007) 2564–2574.
[22] R. Pfoh, A. Li, N. Chakrabarti, J. Payandeh, R. Pomès, E.F. Pai, Structural asymmetry in the magnesium channel CorA points to sequential allosteric regulation, Proc. Natl. Acad. Sci. U. S. A. 109 (2012) 18809–18814.
[23] W. Deng, K. Luo, D. Li, X. Zheng, X. Wei, W. Smith, C. Thammina, L. Lu, Y. Li, Y. Pei, Overexpression of an *Arabidopsis* magnesium transport gene, *AtMGT1*, in *Nicotiana benthamiana* confers Al tolerance, J. Exp. Bot. 57 (2006) 4235–4243.
[24] D.D. Mao, L.F. Tian, L.G. Li, J. Chen, P.Y. Deng, D.P. Li, S. Luan, *AtMGT7*: an *Arabidopsis* gene encoding a low-affinity magnesium transporter, J. Integr. Plant Biol. 50 (2008) 1530–1538.
[25] L.G. Li, L.N. Sokolov, Y.H. Yang, D.P. Li, J. Ting, G.K. Pandy, S. Luan, A mitochondrial magnesium transporter functions in *Arabidopsis* pollen development, Mol. Plant 1 (2008) 675–685.
[26] M.B. Moncrief, M.E. Maguire, Magnesium transport in prokaryotes, J. Biol. Inorg. Chem. 4 (1999) 523–527.
[27] N. Johnsson, A. Varshavsky, Split ubiquitin as a sensor of protein interactions in vivo, Proc. Natl. Acad. Sci. U. S. A. 91 (1994) 10340–10344.
[28] J.P. Miller, R.S. Lo, A. Ben Hur, C. Desmarais, I. Stagljar, W.S. Noble, S. Fields, Large-scale identification of yeast integral membrane protein interactions, Proc. Natl. Acad. Sci. U. S. A. 102 (2005) 12123–12128.
[29] I. Stagljar, C. Korostensky, N. Johnsson, S. te Heesen, A genetic system based on split-ubiquitin for the analysis of interactions between membrane proteins in vivo, Proc. Natl. Acad. Sci. U. S. A. 95 (1998) 5187–5192.
[30] S. Lalonde, A. Sero, R. Pratelli, G. Pilot, J. Chen, M.I. Sardi, S.A. Parsa, D.Y. Kim, B.R. Acharya, E.V. Stein, H.C. Hu, F. Villiers, K. Takeda, Y. Yang, Y.S. Han, R. Schwacke, W. Chiang, N. Kato, D. Loque, S.M. Assmann, J.M. Kwak, J.I. Schroeder, S.Y. Rhee, W.B. Frommer, A membrane protein/signaling protein interaction network for *Arabidopsis* version AMPv2, Front. Physiol. 1 (2010) 24.
[31] A. Roy, A. Kucukural, Y. Zhang, I-TASSER: a unified platform for automated protein structure and function prediction, Nat. Protoc. 5 (2010) 725–738.
[32] Y. Zhang, I-TASSER server for protein 3D structure prediction, BMC Bioinformatics 9 (2008) 40.
[33] C. Grefen, P. Obrdlik, K. Harter, The determination of protein–protein interactions by the mating-based split-ubiquitin system (mbSUS), Methods Mol. Biol. 479 (2009) 217–233.
[34] P. Obrdlik, M. El Bakkoury, T. Hamacher, C. Cappellaro, C. Vilarino, C. Fleischer, H. Ellerbrok, R. Kamuzinzi, V. Ledent, D. Blaudez, D. Sanders, J.L. Revuelta, E. Boles, B. Andre, W.B. Frommer, K^+ channel interactions detected by a genetic system optimized for systematic studies of membrane protein interactions, Proc. Natl. Acad. Sci. U. S. A. 101 (2004) 12242–12247.
[35] R.D. Gietz, R.A. Woods, Transformation of yeast by lithium acetate/single-stranded carrier DNA/polyethylene glycol method, Methods Enzymol. 350 (2002) 87–96.
[36] K. Tamura, J. Dudley, M. Nei, S. Kumar, MEGA4: Molecular Evolutionary Genetics Analysis (MEGA) software version 4.0, Mol. Biol. Evol. 24 (2007) 1596–1599.
[37] K. Tan, A. Sather, J.L. Robertson, S. Moy, B. Roux, A. Joachimiak, Structure and electrostatic property of cytoplasmic domain of ZntB transporter, Protein Sci. 18 (2009) 2043–2052.
[38] Q. Wan, M.F. Ahmad, J. Fairman, B. Gorzelle, F.M. de la, C. Dealwis, M.E. Maguire, X-ray crystallography and isothermal titration calorimetry studies of the *Salmonella* zinc transporter ZntB, Structure 19 (2011) 700–710.
[39] O. Dalmas, L.G. Cuello, V. Jogini, D.M. Cortes, B. Roux, E. Perozo, Structural dynamics of the magnesium-bound conformation of CorA in a lipid bilayer, Structure 18 (2010) 868–878.
[40] N. Chakrabarti, C. Neale, J. Payandeh, E.F. Pai, R. Pomès, An iris-like mechanism of pore dilation in the CorA magnesium transport system, Biophys. J. 98 (2010) 784–792.
[41] K.M. Papp-Wallace, M.E. Maguire, Bacterial homologs of eukaryotic membrane proteins: the 2-TM-GxN family of Mg^{2+} transporters, Mol. Membr. Biol. 24 (2007) 351–356.
[42] J. Hu, M. Sharma, H. Qin, F.P. Gao, T.A. Cross, Ligand binding in the conserved interhelical loop of CorA, a magnesium transporter from *Mycobacterium tuberculosis*, J. Biol. Chem. 284 (2009) 15619–15628.
[43] A.S. Moomaw, M.E. Maguire, Cation selectivity by the CorA Mg^{2+} channel requires a fully hydrated cation, Biochemistry 49 (2010) 5998–6008.
[44] S. Svidová, G. Sponder, R.J. Schweyen, K. Djinovic-Carugo, Functional analysis of the conserved hydrophobic gate region of the magnesium transporter CorA, Biochim. Biophys. Acta 1808 (2011) 1587–1591.
[45] J. Payandeh, C. Li, M. Ramjeesingh, E. Poduch, C.E. Bear, E.F. Pai, Probing structure–function relationships and gating mechanisms in the CorA Mg^{2+} transport system, J. Biol. Chem. 283 (2008) 11721–11733.
[46] J. Chen, S. Lalonde, P. Obrdlik, V.A. Noorani, S.A. Parsa, C. Vilarino, J.L. Revuelta, W.B. Frommer, S.Y. Rhee, Uncovering *Arabidopsis* membrane protein interactome enriched in transporters using mating-based split ubiquitin assays and classification models, Front. Plant Sci. 3 (2012) 124.
[47] P. Obrdlik, M. El Bakkoury, T. Hamacher, C. Cappellaro, B.H. Wu, E. Boles, B. Andre, W.B. Frommer, An optimized split ubiquitin system for systematic identification and characterization of membrane protein interactions, Yeast 20 (2003) S353.
[48] S. Ishijima, Z. Shigemi, H. Adachi, N. Makinouchi, I. Sagami, Functional reconstitution and characterization of the *Arabidopsis* Mg^{2+} transporter AtMRS2-10 in proteoliposomes, Biochim. Biophys. Acta 1818 (2012) 2202–2208.
[49] A. Guskov, N. Nordin, A. Reynaud, H. Engman, A.K. Lundbäck, A.J. Jong, T. Cornvik, T. Phua, S. Eshaghi, Structural insights into the mechanisms of Mg^{2+} uptake, transport, and gating by CorA, Proc. Natl. Acad. Sci. U. S. A. 109 (2012) 18459–18464.
[50] Y. Xia, A.K. Lundbäck, N. Sahaf, G. Nordlund, P. Brzezinski, S. Eshaghi, Co^{2+} selectivity of *Thermotoga maritima* CorA and its inability to regulate Mg^{2+} homeostasis present a new class of CorA proteins, J. Biol. Chem. 286 (2011) 16525–16532.
[51] A. Guskov, S. Eshaghi, The mechanisms of Mg(2+) and Co(2+) transport by the CorA family of divalent cation transporters, Curr. Top. Membr. 69 (2012) 393–414.
[52] M. Wachek, M.C. Aichinger, J.A. Stadler, R.J. Schweyen, A. Graschopf, Oligomerization of the Mg^{2+}-transport proteins Alr1p and Alr2p in yeast plasma membrane, FEBS J. 273 (2006) 4236–4249.
[53] J.M. Lee, R.C. Gardner, Residues of the yeast ALR1 protein that are critical for magnesium uptake, Curr. Genet. 49 (2006) 7–20.
[54] G. Sponder, S. Svidova, R. Schindl, S. Wieser, R.J. Schweyen, C. Romanin, E.M. Froschauer, J. Weghuber, Lpe10p modulates the activity of the Mrs2p-based yeast mitochondrial Mg^{2+} channel, FEBS J. 277 (2010) 3514–3525.
[55] Z.C. Chen, N. Yamaji, R. Motoyama, Y. Nagamura, J.F. Ma, Upregulation of a magnesium transporter gene *OsMGT1* is required for conferring aluminum tolerance in rice, Plant Physiol. 159 (2012) 1624–1633.